

Universal Fluctuation-Response Relations of Nonequilibrium Dynamics: A Trajectory Information Geometry Framework

Jiming Zheng* and Zhiyue Lu†

Department of Chemistry, University of North Carolina-Chapel Hill, NC

(Dated: May 9, 2024)

Unraveling the universal principles governing the response of complex systems to environmental changes is crucial for predicting and controlling their behavior. While fluctuation-dissipation relations have been established for systems near equilibrium, a general framework for understanding the responsiveness of systems far from steady states remains elusive. Here, we introduce a novel approach based on the information geometry of stochastic trajectories to derive a set of universal thermodynamic bounds on the response of any Markov system, regardless of its proximity to steady states. This theory establishes a new paradigm in non-equilibrium statistical mechanics, providing a unified perspective on the behavior of non-stationary systems, from biological processes to engineered devices, and paving the way for designing complex responsiveness in far-from-equilibrium systems.

Introduction.—Unraveling the principles governing the sensitivity and robustness of biological systems to external perturbations is crucial for understanding and designing life-like behaviors in complex systems. While the fluctuation-dissipation theorem [1] captures the response of systems near equilibrium, and recent works have provided general response relations for non-equilibrium steady states (NESS) [2–5], a general framework for understanding the responsiveness of systems far from steady states remains elusive.

A non-stationary theory beyond NESS is essential for understanding realistic biological and thermodynamic processes. For instance, in phenomena such as temperature compensation [6–8], exact adaptation [9–11], fold-change detection [11, 12], and neuronal responses to sensory stimuli [13], systems exhibit strong non-monotonic dynamics that cannot be adequately described by NESS-based approaches. Moreover, in stochastic thermodynamics, systems displaying the Mpemba effect [14–17] further highlight the need for a comprehensive non-stationary response theory.

In this letter, we introduce a novel approach based on the information geometry of stochastic trajectories to derive a set of universal thermodynamic bounds on the response of any Markov system, regardless of its proximity to steady states. Our results go beyond recent non-stationary theories [5, 18, 19] by providing both universal and explicit bounds that specifically relate to the system’s dynamic parameters, such as transition rates, allowing for straightforward evaluation from numerical simulations or experimental observations. This dynamically explicit approach offers a more intuitive understanding of how a system’s dynamics influence its response to perturbations. This universal information geometry framework has the potential to transform our understanding of complex systems and pave the way for the design of highly responsive, far-from-equilibrium systems. The success of the new theory lies in constructing information geometry [20–23] for the space of Markovian

trajectory probability distributions. The key difference between our construction and previous ones[22, 23] is that our geometric structure is constructed for the space of trajectory probability distributions [24].

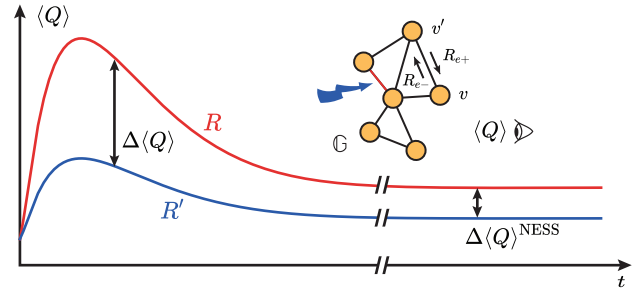


FIG. 1. System’s transient response toward changes to its kinetic rates R and R' can be captured by the difference in the observable’s value at different time t : $\Delta \langle Q \rangle(t) = |\langle Q[X_t] \rangle' - \langle Q[X_t] \rangle|$. This transient response cannot be captured by $\Delta \langle Q \rangle^{\text{NESS}}$, which is obtained by observing the systems at their NESS.

Setup.—Consider a Markov process described by a graph $\mathbb{G} = (\{v_v\}, \{e_e\})$ with N_v vertices $\{v_v\}$ and N_e undirected edges $\{e_e\}$. Every undirected edge e_e is assigned with a pair of forward and reverse directions, with the corresponding transition rates denoted by (R_{e_+}, R_{e_-}) . One can alternatively index the directed rate by a pair of the state indexes (v, v') , or the head and the tail of the directed edge. For instance, if the head and tail of the directed edge e_+ are denoted by $h(e_+) = v'$ and $t(e_+) = v$, then the transition rate from v' to v is $R_{vv'} = R_{e_+}$ (and equivalently $R_{v'v} = R_{e_-}$).

A Markov jump process on the graph \mathbb{G} is described by the Master equation

$$\frac{d\mathbf{p}(t)}{dt} = R \cdot \mathbf{p}(t), \quad (1)$$

where $\mathbf{p}(t) = (p_1(t), \dots, p_{N_v}(t))^T$ is the column vector of probability distributions on vertices at time t and $R =$

$\{R_{vv'}\}_{N_v \times N_v}$ is the rate matrix with diagonal elements $R_{vv} = -\sum_{v', v' \neq v} R_{v'v}$. We assume that the matrix R is irreducible. For illustrative purposes, we also assume that all the transitions are reversible, that is $R_{e+} \neq 0$ only if $R_{e-} \neq 0$.

The geometric structure, one of the central objects in this work, is built on the space of trajectory probabilities. A trajectory with time length τ can be specified by a sequence of n jump events at time $\{t_i\}$:

$$X_\tau = ((x_0, t_0), (x_1, t_1), \dots, (x_n, t_n)), \quad (2)$$

where $x_i \in \{v_v\}$, $t_0 = 0$ is the initial time, and $t_n \leq \tau$ is when is last jump occurs. The probability of the trajectory X_τ is given by $\mathcal{P}[X_\tau] = \mathcal{P}[X_\tau|x_0]p_{x_0}(0)$ where $\mathcal{P}[X_\tau|x_0]$ is the conditional path probability of X_τ with the given initial state x_0 . It is given by the products of transition probabilities and dwelling probabilities [25]

$$\mathcal{P}[X_\tau|x_0] = \prod_{i=0}^{n-1} R_{x_i x_{i+1}} \prod_{i=0}^n e^{\int_{t_i}^{t_{i+1}} R_{x_i x_i} dt}, \quad (3)$$

where $t_{n+1} = \tau$ is the time length of the trajectory.

To describe the influence of environmental change or external stimuli, we introduce a general parameterization $R(\boldsymbol{\xi})$ using a column vector

$$\boldsymbol{\xi} = (\xi_1, \dots, \xi_{N_p})^\top \quad (4)$$

with N_p control parameters. Here the vector $\boldsymbol{\xi}$ represents externally controlled parameters, such as environmental variables including temperature, pressure, pH, chemical concentration, electric field, etc. In this description, alternation in the control parameters $\boldsymbol{\xi}$ may result in changes in the system's dynamics $R(\boldsymbol{\xi})$'s, which may further lead to changes in the probability distributions of stochastic trajectories $\mathcal{P}[X_\tau]$'s and thus the observable $Q[X_\tau]$.

The central results of this letter capture the responsiveness of arbitrary Markov systems in terms of universal inequalities for the changes in the trajectory-averaged observable $\langle Q[X_\tau] \rangle$. Here the angular brackets denote an average over the ensemble of trajectories generated from the rate matrix $R(\boldsymbol{\xi})$. We consider two types of responses: (1) *perturbative response*, $|\partial_{\xi_p} \langle Q \rangle|$, which captures the change in the non-stationary output observable under infinitesimal environmental differences, and (2) *finite response*, $|\langle Q \rangle' - \langle Q \rangle|$, which quantifies the difference in non-stationary outputs between two finitely different environmental conditions $\boldsymbol{\xi}'$ and $\boldsymbol{\xi}$.

Information geometric structure for conditional path probabilities.—To build a general theory, we construct information geometry [20, 21] for the space of trajectory probabilities, where the Fisher information matrix is chosen as the metric tensor for the parametric probability distributions.

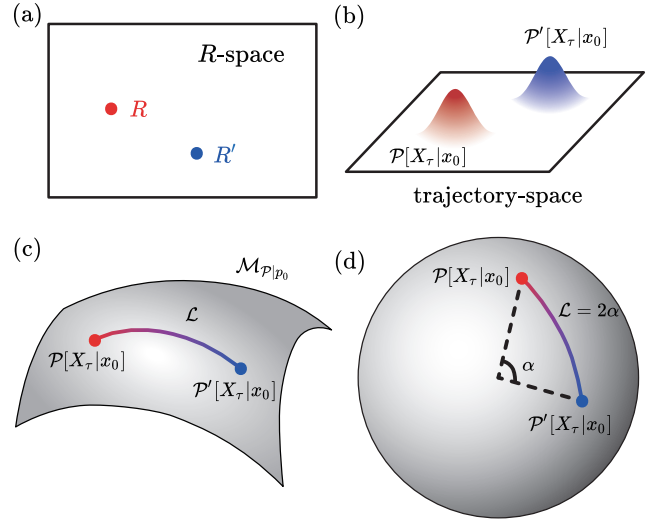


FIG. 2. Relations between four spaces to capture non-stationary Markov Processes. (a) The space of all possible probability rate matrices. (b) In the trajectory space, illustrated are two probability distributions of trajectories conditioned on the initial distribution $\mathbf{p}(0)$. Each distribution corresponds to one Markov process (rate matrix R). (c) Trajectory probability manifold, where each point is a distinct conditional probability distribution of trajectories, which corresponds to one distinct rate matrix R . (d) The trajectory probability manifold can be isometrically embedded to a hypersphere of radius 2, and the geodesic between two trajectory probability distributions becomes the arc length between the two points on the hypersphere.

Consider the manifold $\mathcal{M}_{\mathcal{P}|p_0}$ of conditional path probabilities $\mathcal{P}[X_\tau|x_0]$ with a certain given initial distribution $\mathbf{p}(0)$ whose elements $p_i(0)$ are all positive. Conditioned on an initial distribution $\mathbf{p}(0)$, one can uniquely determine the trajectory ensemble from the rate matrix $R(\boldsymbol{\xi})$, as shown in Fig. 2(a)(b). Thus, for a given graph \mathbb{G} , the set of parameters $\{\xi_p\}$ servers as a coordinate system on $\mathcal{M}_{\mathcal{P}|p_0}$. Since the degree of freedom for R is $2N_e$, the resulting conditional path probabilities lie on a $2N_e$ -dimensional manifold, shown in Fig. 2(c). Every point on the manifold uniquely specifies an evolution process (i.e., a distribution of trajectories).

A natural and complete choice of the coordinate system on $\mathcal{M}_{\mathcal{P}|p_0}$ is the set of all transition rates $\{R_{e+}\} \cup \{R_{e-}\}$. With the help of the trajectory KL divergence in the recent work [24], we derive the *first main result*, the explicit expression for the Fisher information metric:

$$g(\{R_{e+}\}, \{R_{e-}\}) = \text{diag} \left\{ \left\{ \frac{\mathcal{A}_{e+}}{R_{e+}^2} \right\}, \left\{ \frac{\mathcal{A}_{e-}}{R_{e-}^2} \right\} \right\}. \quad (5)$$

where we use $\mathcal{A}_{e+} = \int_0^\tau R_{e+} p_{h(e+)}(t) dt$ to denote the *directed activity* (i.e. time-integrated direct traffic) on the directed edge $e+$. [26] The directed activity is the expectation value of the number of directed transitions along edge $e+$ within time duration τ [27], which was shown to

play an important role in various thermodynamic relations by recent studies [28–33]. The global diagonal form of the metric tensor implies that $\boldsymbol{\xi} = (\{R_{e+}\}, \{R_{e-}\})$ is a set of orthogonal basis everywhere. Taking advantage of the simple form, it is straightforward to calculate other geometric quantities. For example, the line element ds^2 in terms of transition rates is then given by

$$ds^2 = \sum_{e+} \frac{\mathcal{A}_{e+}}{R_{e+}^2} dR_{e+}^2 + \sum_{e-} \frac{\mathcal{A}_{e-}}{R_{e-}^2} dR_{e-}^2. \quad (6)$$

For a infinitesimal perturbation along a certain axis R_{e+} of the local coordinates, the line element is simply $ds^2 = \frac{\mathcal{A}_{e+}}{R_{e+}^2} dR_{e+}^2$. This line element can be considered as an infinitely short segment on the manifold shown in Fig. 2(c). The metric under other coordinate systems can be obtained from coordinate transformations.

The information geometric structure provides a geometric-based method to analyze Markov processes on the trajectory level that can be potentially applied to various systems (e.g. non-stationary processes and time-dependently driven processes). In this work, we apply it to the analysis of infinitesimal and finite perturbations for arbitrary non-stationary Markov processes.

Transition rate perturbations.—To proceed, we apply the Cramér-Rao inequality [34, 35] on the trajectory Fisher information metric in Eq. (5). It immediately yields the *second main result* of this work – the thermodynamic bound for the response magnitude of any quantity Q to the perturbation of the rate of a directed edge:

$$|\partial_{R_{e\pm}} \langle Q \rangle| \leq \sqrt{\text{Var}[Q]} \cdot \frac{\sqrt{\mathcal{A}_{e\pm}}}{R_{e\pm}}, \quad (7)$$

where the average $\langle \dots \rangle$ is taken over all length- τ trajectories and $\text{Var}[Q] = \langle Q^2 \rangle - \langle Q \rangle^2$ is the variance of Q on the trajectory level. (See SI.III.) The perturbation can be applied on any directed rate $R_{e\pm} \in \{R_{e+}\} \cup \{R_{e-}\}$ as the choice of forward and reverse directions is arbitrary. Notice that this thermodynamic bound can be applied to general non-stationary processes far away from NESS. In general, Eq. (7) implies that the directed edge with larger activities may allow for a stronger response toward the perturbation of its rate.

To illustrate the result, we demonstrate the responsiveness of three types of quantities $\langle Q \rangle$: (i) state probability $p_v(t)$, (ii) current $j_e(t) = R_{e+}p_{h(e+)} - R_{e-}p_{h(e-)}$, which is time-asymmetric, and (iii) traffic $t_e(t) = R_{e+}p_{h(e+)} + R_{e-}p_{h(e-)}$, which is time-symmetric [27].

(i) Responsiveness of state probability. The transient probability distributions $p_{v_0}(t)$ on the vertex v_{v_0} at time t can be obtained from $\langle \delta_{v(t), v_0} \rangle$, where

$$\delta_{v(t), v_0} = \begin{cases} 1, & v(t) = v_0, \\ 0, & \text{otherwise.} \end{cases} \quad (8)$$

The Kronecker delta picks out all the trajectories on the vertex v_{v_0} at time t . Taking advantage of the fact that

$\delta_{v(t), v_0}^2 = \delta_{v(t), v_0}$, we can further calculate the variance of the observable as $\text{Var}[\delta_{v(t), v_0}] = p_{v_0}(t)[1 - p_{v_0}(t)]$. Therefore, the thermodynamic bound for the state probability $p_{v_0}(t)$'s response to the perturbation of the rate of a certain edge $e\pm$ is

$$|\partial_{R_{e\pm}} p_{v_0}| \leq \sqrt{p_{v_0}(1 - p_{v_0})} \cdot \frac{\sqrt{\mathcal{A}_{e\pm}}}{R_{e\pm}}. \quad (9)$$

The responsiveness inequality holds for any initial distribution $\mathbf{p}(0)$, arbitrary vertex v_{v_0} , and perturbed edge $e\pm$. It also holds for any time τ . The upper bound approaches zeros for $\tau \rightarrow 0$ since the probability hasn't evolved yet and no jump occurs on the edge $e+$. Notably, the upper bound is determined only by quantities related to the perturbed directed edge $e\pm$ and the observed vertex v_{v_0} and is irrelevant to all other vertices and edges. Since the right-hand side of Eq. (9) scales with $\mathcal{O}(1/\sqrt{R_{e\pm}})$, it implies that the probability of a given state is more responsive to perturbations on those edges of smaller rates and less responsive to perturbations on the edges of larger rates. See Fig. 3 (a) for numerical verification of the theory.

(ii) Responsiveness of current and (iii) Responsiveness of traffic. By applying the similar analysis to current-like and traffic-like observables, we obtain the non-stationary thermodynamic bounds for the responsiveness of j_{e_0} and t_{e_0} :

$$|\partial_{R_{e\pm}} j_{e_0}| \leq \sqrt{\mathfrak{I}_{e_0} - j_{e_0}^2} \cdot \frac{\sqrt{\mathcal{A}_{e\pm}}}{R_{e\pm}}, \quad (10a)$$

$$|\partial_{R_{e\pm}} t_{e_0}| \leq \sqrt{\mathfrak{I}_{e_0} - t_{e_0}^2} \cdot \frac{\sqrt{\mathcal{A}_{e\pm}}}{R_{e\pm}}, \quad (10b)$$

where $\mathfrak{I}_e = R_{e+}^2 p_{h(e+)} + R_{e-}^2 p_{h(e-)}$ is a second order traffic on the edge e . Still, the upper bounds only depend on quantities related to the perturbed edge and the observed edge. As the right-hand side of Eqs. (10a) and (10b) scales with $\mathcal{O}(\sqrt{R_{e\pm}})$, perturbations on edges with larger transition rates would allow larger responses on current and traffic. See Fig. 3 (b) and (c) for numerical verification of the theory.

Coordinate Transformation.—In the above analysis, we discussed the system's responses to the perturbation of one directed transition rate. Here we illustrate the responsiveness theory in a different coordinate system. The new coordinate system may be defined by the set of controlled parameters $\boldsymbol{\xi}$ defined in Eq. (4). To better illustrate the system's response to the changes of thermodynamic driving force, we choose a coordinate system that separately treats the symmetric and asymmetric parts of the transition rates on each edge. In stochastic thermodynamics, the forward and backward transition rates on an edge e can be parameterized by symmetric $R_e = \sqrt{R_{e+}R_{e-}}$ and asymmetric $A_e = \ln(R_{e+}/R_{e-})$ parts. The asymmetric part A_e is the thermodynamic

$$|p'_{v_0} - p_{v_0}| \leq \sin^*(G_{e\pm}), \quad (14a)$$

$$|j'_{e_0} - j_{e_0}| \leq 2 \max\{R_{e_0+}, R_{e_0-}\} \cdot \sin^*(G_{e\pm}), \quad (14b)$$

$$|t'_{e_0} - t_{e_0}| \leq \max\{R_{e_0+}, R_{e_0-}\} \cdot \sin^*(G_{e\pm}). \quad (14c)$$

See Fig. 3 (d)-(f) for numerical verification of the theory.

Discussions.—In summary, this work presents a set of universal fluctuation-response inequalities that govern the response of non-stationary processes to both infinitesimal and finite perturbations. Our results provide a powerful tool for understanding and predicting the behavior of complex systems far from equilibrium, with potential applications ranging from biological processes to engineered devices. These results provide a unified framework for predicting and optimizing the responsiveness of stochastic systems, enabling the design of environmental sensitivity and non-monotonic responsiveness into complex biological and engineered systems. This geometric approach lays the foundation for uncovering the fundamental principles governing complex systems far from equilibrium, opening up new avenues for research across diverse fields, from biophysics to materials science

The unique theoretical framework is based on an information geometric structure on the manifold of conditional Markovian trajectory distributions. This new framework is inherently different from some previous results [22, 23, 38, 39], since the previous results describe the manifold \mathcal{M}_p of the probability distributions of states, whereas the new geometry in this work is built on $\mathcal{M}_{\mathcal{P}|p_0}$, the manifold of conditional distribution of trajectories. The manifold of complete trajectory probability distributions $\mathcal{P}[X_\tau]$ is locally the product manifold $\mathcal{M}_p \times \mathcal{M}_{\mathcal{P}|p_0}$ and its metric is the product metric $g_p \oplus g_{\mathcal{P}|p_0}$. In this work, the reversibility of matrix R is not necessary for the geometric structure. Setting some rates to zero reduces the dimension of the manifold. In this case, the coordinate transformation to the symmetric/asymmetric parameters holds only for part of the edges. Moreover, we do not need to include the length of trajectories, τ , as a parameter. It is because the rates ($\{R_{e+}\}, \{R_{e-}\}$) and the time length τ are dependent due to the equivalence relation shown in recent works [40]. The saturation condition for the bounds are discussed in SI.V.

It is noteworthy that the result Eq. (5) based on the Fisher Information of classical Markov trajectories agrees with the previous work based on the quantum Fisher Information obtained from the Lindblad equation [41, 42]. In the future, it is useful to explore if the information geometric framework developed for classical Markov systems in this work, including the non-perturbative responsiveness bound as Eq. (13a) can be extended to Lindbladian systems.

Acknowledgments.— We acknowledge the financial support from National Science Foundation Grant DMR-

2145256.

* jiming@unc.edu

† zhiyuelu@unc.edu

- [1] R. Kubo, The fluctuation-dissipation theorem, Reports on progress in physics **29**, 255 (1966).
- [2] J. A. Owen, T. R. Gingrich, and J. M. Horowitz, Universal thermodynamic bounds on nonequilibrium response with biochemical applications, Physical Review X **10**, 011066 (2020).
- [3] T. Aslyamov and M. Esposito, Nonequilibrium response for markov jump processes: Exact results and tight bounds, Physical Review Letters **132**, 037101 (2024).
- [4] T. Aslyamov and M. Esposito, A general theory of static response for markov jump processes, arXiv preprint arXiv:2402.13990 (2024).
- [5] P. E. Harunari, S. D. Cengio, V. Lecomte, and M. Poletini, Mutual linearity of nonequilibrium network currents, arXiv preprint arXiv:2402.13193 (2024).
- [6] P. D. Gould, J. C. Locke, C. Larue, M. M. Southern, S. J. Davis, S. Hanano, R. Moyle, R. Milich, J. Putterill, A. J. Millar, *et al.*, The molecular basis of temperature compensation in the arabidopsis circadian clock, The Plant Cell **18**, 1177 (2006).
- [7] P. B. Kidd, M. W. Young, and E. D. Siggia, Temperature compensation and temperature sensation in the circadian clock, Proceedings of the National Academy of Sciences **112**, E6284 (2015).
- [8] H. Fu, C. Fei, Q. Ouyang, and Y. Tu, Temperature compensation through kinetic regulation in biochemical oscillators, arXiv preprint arXiv:2401.13960 (2024).
- [9] U. Alon, M. G. Surette, N. Barkai, and S. Leibler, Robustness in bacterial chemotaxis, Nature **397**, 168 (1999).
- [10] T.-M. Yi, Y. Huang, M. I. Simon, and J. Doyle, Robust perfect adaptation in bacterial chemotaxis through integral feedback control, Proceedings of the National Academy of Sciences **97**, 4649 (2000).
- [11] U. Alon, *An introduction to systems biology: design principles of biological circuits* (Chapman and Hall/CRC, 2019).
- [12] L. Goentoro, O. Shoval, M. W. Kirschner, and U. Alon, The incoherent feedforward loop can provide fold-change detection in gene regulation, Molecular cell **36**, 894 (2009).
- [13] P. Dayan and L. F. Abbott, *Theoretical neuroscience: computational and mathematical modeling of neural systems* (MIT press, 2005).
- [14] Z. Lu and O. Raz, Nonequilibrium thermodynamics of the markovian mpemba effect and its inverse, Proceedings of the National Academy of Sciences **114**, 5083 (2017).
- [15] I. Klich, O. Raz, O. Hirschberg, and M. Vucelja, Mpemba index and anomalous relaxation, Physical Review X **9**, 021060 (2019).
- [16] S. S. Chittari and Z. Lu, Geometric approach to nonequilibrium hasty shortcuts, The Journal of Chemical Physics **159** (2023).
- [17] G. Teza, R. Yaacoby, and O. Raz, Relaxation shortcuts through boundary coupling, Physical review letters **131**, 017101 (2023).

- [18] A. Dechant and S.-i. Sasa, Fluctuation–response inequality out of equilibrium, *Proceedings of the National Academy of Sciences* **117**, 6430 (2020).
- [19] C. Maes, Response theory: a trajectory-based approach, *Frontiers in Physics* **8**, 229 (2020).
- [20] S.-i. Amari, *Information geometry and its applications*, Vol. 194 (Springer, 2016).
- [21] N. Ay, J. Jost, H. Vân Lê, and L. Schwachhöfer, *Information geometry*, Vol. 64 (Springer, 2017).
- [22] S. Ito, Stochastic thermodynamic interpretation of information geometry, *Physical review letters* **121**, 030605 (2018).
- [23] G. E. Crooks, Measuring thermodynamic length, *Physical Review Letters* **99**, 100602 (2007).
- [24] A. Pagare, Z. Zhang, J. Zheng, and Z. Lu, Stochastic distinguishability of Markovian trajectories, *The Journal of Chemical Physics* **160**, 171101 (2024).
- [25] U. Seifert, Stochastic thermodynamics, fluctuation theorems and molecular machines, *Reports on progress in physics* **75**, 126001 (2012).
- [26] For systems evolving under time-dependent rate matrix, the Fisher Information is discussed in the SI.I.
- [27] C. Maes, Frenesy: Time-symmetric dynamical activity in nonequilibria, *Physics Reports* **850**, 1 (2020).
- [28] M. Baiesi, C. Maes, and B. Wynants, Fluctuations and response of nonequilibrium states, *Physical review letters* **103**, 010602 (2009).
- [29] J. P. Garrahan, Simple bounds on fluctuations and uncertainty relations for first-passage times of counting observables, *Physical Review E* **95**, 032134 (2017).
- [30] I. Di Terlizzi and M. Baiesi, Kinetic uncertainty relation, *Journal of Physics A: Mathematical and Theoretical* **52**, 02LT03 (2018).
- [31] N. Shiraishi, K. Funo, and K. Saito, Speed limit for classical stochastic processes, *Physical review letters* **121**, 070601 (2018).
- [32] P. E. Harunari, A. Dutta, M. Poletti, and É. Roldán, What to learn from a few visible transitions’ statistics?, *Physical Review X* **12**, 041026 (2022).
- [33] Y. Hasegawa, Thermodynamic correlation inequality, *Physical Review Letters* **132**, 087102 (2024).
- [34] C. R. Rao, Information and the accuracy attainable in the estimation of statistical parameters, in *Breakthroughs in Statistics: Foundations and basic theory* (Springer, 1992) pp. 235–247.
- [35] H. Cramér, *Mathematical methods of statistics*, Vol. 26 (Princeton university press, 1999).
- [36] C. Maes, Local detailed balance, *SciPost Physics Lecture Notes* , 032 (2021).
- [37] D. Chandler, *Introduction to modern statistical, Mechanics*. Oxford University Press, Oxford, UK **5**, 449 (1987).
- [38] D. A. Sivak and G. E. Crooks, Thermodynamic metrics and optimal paths, *Physical review letters* **108**, 190602 (2012).
- [39] S. Ito, Geometric thermodynamics for the fokker–planck equation: stochastic thermodynamic links between information geometry and optimal transport, *Information Geometry* **7**, 441 (2024).
- [40] Y. Hasegawa, Unifying speed limit, thermodynamic uncertainty relation and heisenberg principle via bulk-boundary correspondence, *Nature Communications* **14**, 2828 (2023).
- [41] K. Macieszczak, M. Guță, I. Lesanovsky, and J. P. Garrahan, Dynamical phase transitions as a resource for quantum enhanced metrology, *Physical Review A* **93**, 022103 (2016).
- [42] J. P. Garrahan and M. Guta, private communication.